molecular pharmaceutics

Article

Cite This: Mol. Pharmaceutics XXXX, XXX, XXX−XXX

Regulating the Uptake of Viral Nanoparticles in Macrophage and Cancer Cells via a pH Switch

Hamilton Lee,[†,⊥] Candace E. Benjamin,[†,⊥] Chance M. Nowak,[§] Lana H. Tuong,[†] Raymond P. Welch,[†] Zhuo Chen,[†] Madushani Dharmarwardana,[†] Kyle W. Murray,[†] Leonidas Bleris,[‡] Sheena D'Arcy,[†,§] and Jeremiah J. Gassensmith*[,†,‡]

[†]Department of Chemistry and Biochemistry, [‡]Department of Bioengineering, [§]Department of Biological Sciences, The University of Texas at Dallas, Richardson, TX 75080, United States

Supporting Information

ABSTRACT: Controlling the uptake of nanomaterials into phagocytes is a challenging problem. We describe an approach to inhibit the cellular uptake by macrophages and HeLa cells of nanoparticles derived from bacteriophage Qβ by conjugating negatively charged terminal hexanoic acid moieties onto its surface. Additionally, we show hydrazone linkers can be installed between the surface of Qβ and the terminal hexanoic acid moieties, resulting in a pH-responsive conjugate that, in acidic conditions, can release the terminal hexanoic acid moiety and allow for the uptake of the Qβ nanoparticle. The installation of the "pH switch" did not change the structure−function properties of the hexanoic acid moiety and the uptake of the Qβ conjugates by macrophages.

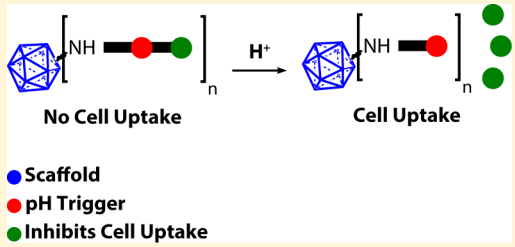

KEYWORDS: *nanomaterials, phagocytes, cellular uptake, Qβ, macrophages*

INTRODUCTION

Nanoparticles have played a key role in various fields of biomedical research in the last few decades for a wide array of applications.[1−5] While the amount of research in this area has been significant, the specific mechanisms behind the cellular uptake of nanoparticles and the particular parameters required to modulate uptake are still not fully understood.[6−8] It has been widely demonstrated[6,7,9−15] that factors, including the size, shape, charge, and hydrophobicity of nanoparticles, significantly affect the uptake of nanoparticles by cells. Specifically, the surface charge of nanoparticles has been considered a critical factor for applications involving imaging and drug delivery.[7]

The surface charge of nanoparticles has been shown to affect nanoparticle uptake by cells largely, but not solely, through nonspecific electrostatic interactions between the charged moieties on the nanoparticle and phospholipid head groups or protein domains on the membrane of the cell.[9,11,16,17] The implication of this view is that nanoparticles with positive surface charges are more favored for uptake by cells, while nanoparticles with negative surface charges are less favored for uptake. This fact has been exploited elegantly by a number of researchers to alter cell uptake in a variety of mammalian cell types.[11,17−22] Although different cell lines react to surface charges of nanoparticles in varying degrees, the previous statement generally holds true across cell types with the exception of phagocytes. Macrophages have been shown to favor the uptake of negatively charged nanoparticles to that of positively charged particles.[23,24] This observation has been explained by fact that macrophages are known to phagocytose negatively charged cells, such as bacteria, and are thus expected to favor the uptake of negatively charged particles.[25] Consequently, reports on controlling the uptake of nanoparticles in macrophages are rare and would be of considerable value for researchers. Macrophages are a type of phagocytic cell that is responsible for clearing foreign materials from the body by shunting them into the organs of the mononuclear phagocyte system, like the liver and kidneys for excretion. Consequently, this recognition and disposal system can potentially reduce the circulatory half-life of nanotherapeutics preventing them from reaching their targets. On the other hand, selective stimulation of the immune system in the context of vaccine development, wound treatment, or targeting infections by controlling when and where the innate immune system is active would be of significant therapeutic interest for researchers in areas from wound treatment to cancer immunotherapy.

Modulating the uptake ability of nanoparticles by switching the surface charge from negative to positive has been an approach to controlling their uptake until a specific stimulus is triggered.[18,19,26] This charge inversion strategy holds potential for increasing the safety and efficacy of existing payload delivery systems by increasing the selectivity of nanoparticle uptake by the intended cells. We set out to utilize this strategy using the virus-like particle (VLP) Qβ as a scaffold for which charged

Special Issue: Click Chemistry for Medicine and Biology

Received: April 1, 2018
Revised: May 15, 2018
Accepted: May 22, 2018
Published: May 22, 2018

DOI: 10.1021/acs.molpharmaceut.8b00348
Mol. Pharmaceutics XXXX, XXX, XXX−XXX

small molecules could be conjugated to reversibly modify cell uptake properties in macrophage models. Our charge inversion strategy relies on acidic environments as a trigger, but we are not pursuing the use of this system in tumor microenvironments, which are not sufficiently acidic. Instead, we are focusing on tissue injuries, where the extracellular pH can be as low as 4.[27−29]

In this article, we highlight our investigations regarding the uptake of our Qβ conjugates by RAW 264.7 macrophages and HeLa cells. We show that we can reversibly alter the uptake properties relative to unfunctionalized Qβ when the terminal moiety is hexanoic acid. We also demonstrate that the hydrazone linker in our hydrazone-based Qβ conjugates hydrolyze when incubated in acidic conditions, allowing for the pH-mediated cell uptake of those conjugates. Our findings suggest that when the size and shape of Qβ nanoparticles are controlled for, the conjugation of a negatively charged terminal hexanoic acid moiety onto the surface of Qβ significantly affects its uptake characteristics by both macrophages and cancer cells.

RESULTS AND DISCUSSION

VLPs offer the advantages of being monodisperse, highly functionalizable, and biodegradable when compared to silica, polymeric, or metallic nanoparticles.[30−36] VLPs are self-assembled macromolecular structures composed of tens to thousands of individual protein subunits.[37] The particular VLP utilized in this article is bacteriophage Qβ, a 28 nm icosahedral protein nanoparticle with a capsid composed of 180 identical coat proteins. These coat proteins self-assemble around ssRNA and are linked together via disulfide bonds between the Cys74 and Cys80 residues of each coat protein. Each 14.1 kDa coat protein is composed of 132 amino acids, with four of these residues, the N-terminus Ala1, Lys2, Lys13, and Lys46, being solvent exposed and featuring primary amines available for functionalization (Scheme 1a).[30,38] The ease of synthetic modification and its resilience against heat and solvent have allowed Qβ to emerged as a workhorse in VLP nanotechnology as a promising candidate in vaccine and immunotherapeutic applications, making it an excellent model for our study.[30,39−41]

The exposed primary amines were utilized for the conjugation of terminal carboxylate moieties to provide a negative charge to the surface of Qβ. To keep our analysis simple, we started with a hexanoic acid derivative. To that end, 6-(prop-2-yn-1-yloxy)hexanoic acid (6X) was conjugated to the solvent exposed lysine residues on the surface of Qβ. We also prepared a trimesic acid (Trim) derivative under the assumption that two negative charges should be more effective than one, and both syntheses are illustrated in Scheme 1B. These two conjugates were characterized by MALDI-TOF mass spectrometry, transmission electron microscopy (TEM), and dynamic light scattering (DLS) and were found to have retained the characteristic morphology of the underlying VLP (Figure 1). MALDI-TOF revealed that an average of two modifications per coat protein occurred with both derivatives. Native agarose gel electrophoresis showed a clear band shift of the conjugates toward the positive electrode despite being modestly larger, suggesting that the overall charge of the VLP had become more negative for both conjugates.

We prepared conjugates using Qβ internally loaded with green fluorescent protein (Q$\beta_{(GFP)}$) to provide a fluorescent tag[42] for imaging studies. Both conjugates were incubated in the presence of animal serum with HeLa and RAW 264.7 macrophage cells. To our surprise, the conjugates behaved

Scheme 1. (A) Structure of Qβ[a] and (B) Synthesis of Both Conjugates Qβ-6X and Qβ-Trim[b]

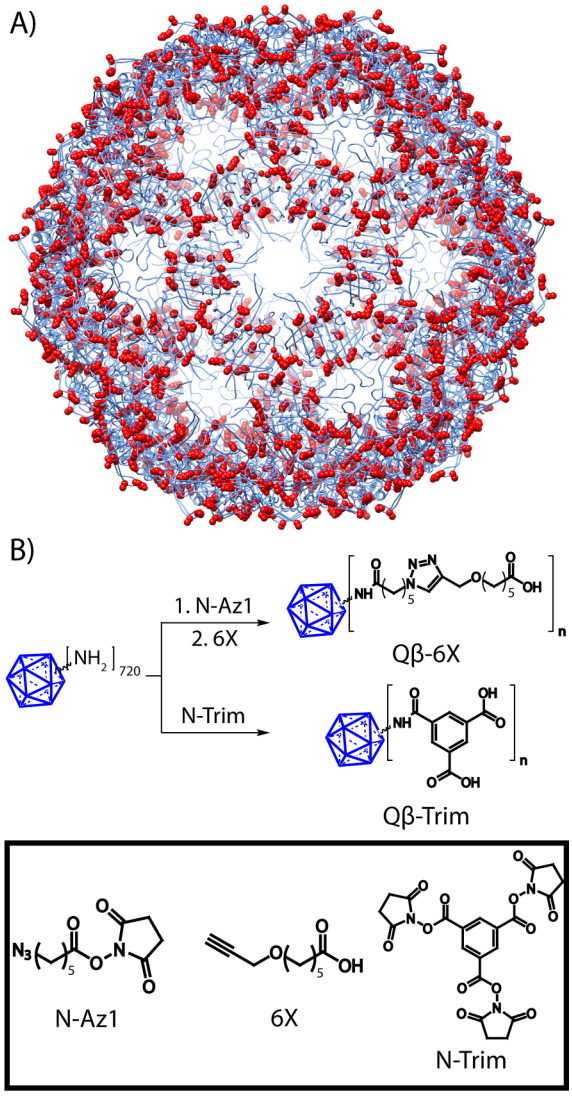

[a]Red spheres correspond to primary amines. [b]Blue icosahedron represents Qβ.

quite differently. According to flow cytometry analysis, shown in Figure 2, the cellular uptake of Q$\beta_{(GFP)}$-6X was inhibited while the uptake of Q$\beta_{(GFP)}$-Trim was not, despite trimesic acid having an additional negative charge. To our knowledge, hexanoic acid does not have a specific receptor that mediates the uptake of nanoparticles by cells, though a review of the literature[43] done after our experiment suggested that derivatives of benzoic acid, which we believe our conjugate most closely resembles, do.

With these results in hand, we next sought to introduce a stimuli responsive switch between the capsid and the hexanoic acid moiety. This would accomplish two objectives: (1) it would demonstrate that the linkage between the hexanoic acid and the VLP is amenable to modification without altering the structure−property relationship, and (2) it would provide a proof-of-principle example of using "charge flipping" to alter uptake behavior. To that end, we designed a hydrazone linkage, which is cleavable under the acidic pH typically found in the skin or in wounds, where immune activation by a vaccine adjuvant would likely be most efficacious.[27−29] Hydrazones

DOI: 10.1021/acs.molpharmaceut.8b00348
Mol. Pharmaceutics XXXX, XXX, XXX−XXX

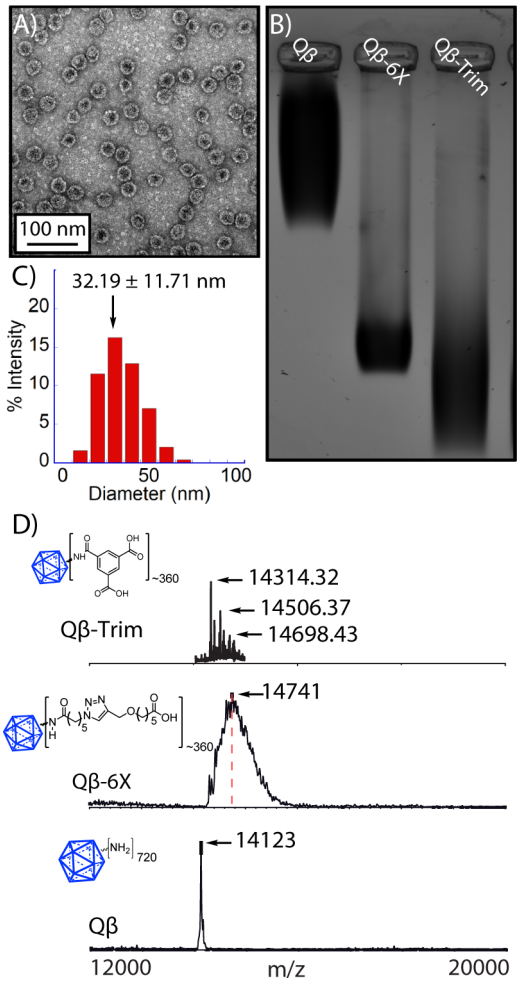

Figure 1. (A) TEM image of Qβ-6X. (B) Native agarose gel electrophoresis of Qβ, Qβ-6X, and Qβ-Trim. The greater mobility toward the positive electrode (bottom) suggests an increase in negative charge. (C) Dynamic light scattering data of Qβ-6X. (D) MALDI-TOF mass spectra of Qβ and Qβ-6X showing observed masses. ESI-TOF mass spectrum of Qβ-Trim showing one, two, and three functionalized residues per coat protein.

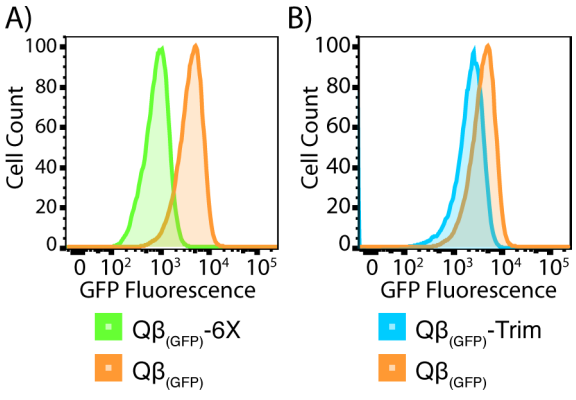

Figure 2. Representative histogram from flow cytometry studies corresponding to RAW 264.7 macrophages incubated with their respective Q$\beta_{(GFP)}$ samples at 40 μM. All cells were incubated with the Qβ conjugates for 4 h at 37 °C.

have been frequently used for their ability to hydrolyze in mildly acidic conditions and, in particular, for cargo release from nanoparticles inside endosomes.[30,44−46] These pH ranges are compatible with the Qβ VLP.[47] In addition, the resulting terminal hydrazine moiety, after the cleavage of the hydrazone bond, should form a cationic hydrazinium ion following protonation in water.

We thus created two hydrazone analogues of hexanoic acid to test their efficacy as a pH-mediated switch. Conjugation of the hydrazone switch is shown in Scheme 2. We varied the hydrazone linker length by using both 1-chloropropan-2-one and 1-chloropentanone. Briefly, an NHS-ester containing hydrazone and azide functionalities was attached to 6X in situ via a copper catalyzed azide−alkyne cycloaddition (CuAAC). A solution of Qβ was added and after completion of the reaction, the resulting conjugate was purified via centrifuge filtration. As shown in Figures 3a,c and S7, the resulting conjugates maintain their spherical morphology.

Scheme 2. Synthesis of Qβ-Z Conjugates[a]

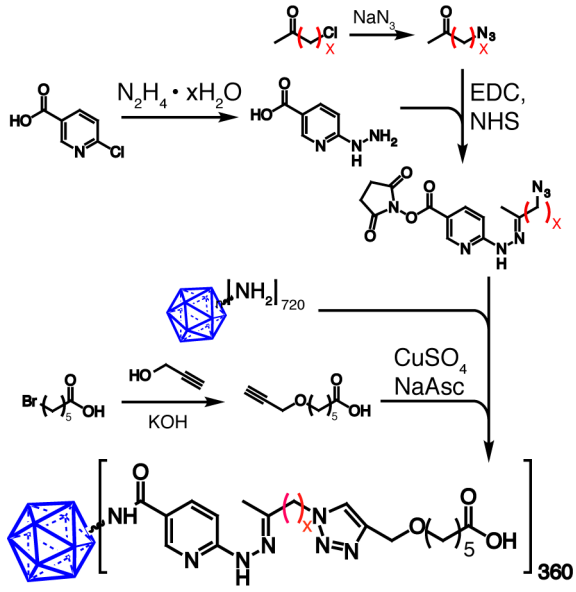

[a]The use of 1-chloropropan-2-one (X = 1) as a starting material results in Qβ-ZX. The use of 5-chloropentan-2-one (X = 3) results in Qβ-ZX2.

The electrophoretic mobility of proteins can be used to approximate their relative surface charge given that their size and morphologies are similar. The effect of the terminal carboxylic acid moieties on the surface charge of the Qβ conjugates was evaluated via native agarose gel electrophoresis. A representative gel comparing the electrophoretic mobility of unfunctionalized Qβ to Qβ conjugates, including both the hexanoic acid-terminated hydrazone (ZX) as well as the hydrolyzed version of the same (ZX-Hyd), is shown in Figure 3b. Unsurprisingly, all the anionic conjugates show greater electrophoretic mobility than the unfunctionalized Qβ sample. To test the efficacy of the hydrazone switch, the Qβ-Z conjugates were incubated in MES buffer (0.1 M, pH 5.0) for 48 h. The electrophoretic mobilities of the Qβ-ZX-Hyd conjugates were reduced relative to the Qβ-Z conjugates that had not undergone incubation in acidic conditions. It is not clear why the putatively protonated hydrolyzed hydrazine conjugates did not retreat to approximately the same position as the unfunctionalized Qβ. ESI-TOF data (Figure S5) show the predicted mass of the hydrolyzed product.

DOI: 10.1021/acs.molpharmaceut.8b00348
Mol. Pharmaceutics XXXX, XXX, XXX−XXX

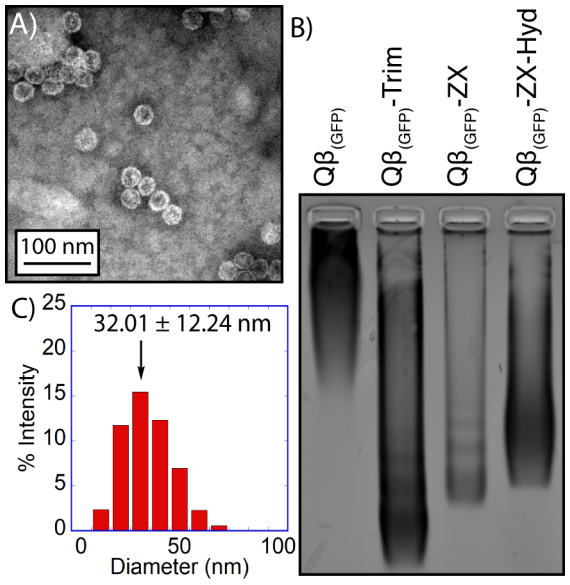

Figure 3. (A) TEM micrograph of the Q$\beta_{(GFP)}$-ZX conjugate. (B) Native agarose gel electrophoresis showing Qβ, Qβ conjugates, and the hydrolyzed product Qβ-ZX-Hyd. (C) DLS measurement of the Q$\beta_{(GFP)}$-ZX conjugate showing a uniform size distribution. The measurements were taken in KP buffer (0.1 M, pH 7.4, 25 °C) at concentrations of ~1 mg/mL.

The kinetics of the hydrazone hydrolysis were investigated using fluorescence spectroscopy, since the Qβ conjugates may hold potential for therapeutic applications involving the delivery of payloads to specific targets. Although hydrazones reliably hydrolyze in mildly acidic conditions, the local chemical environment may affect the rate of hydrolysis. Qβ-ZFITC (Figure 4a), a Qβ conjugate containing a terminal FITC moiety and a hydrazone linker, was synthesized for this study.

The fluorescence of FITC (λ_{Ex} = 450 nm; λ_{Em} = 520 nm) and other fluorescein derivatives are known to self-quench at

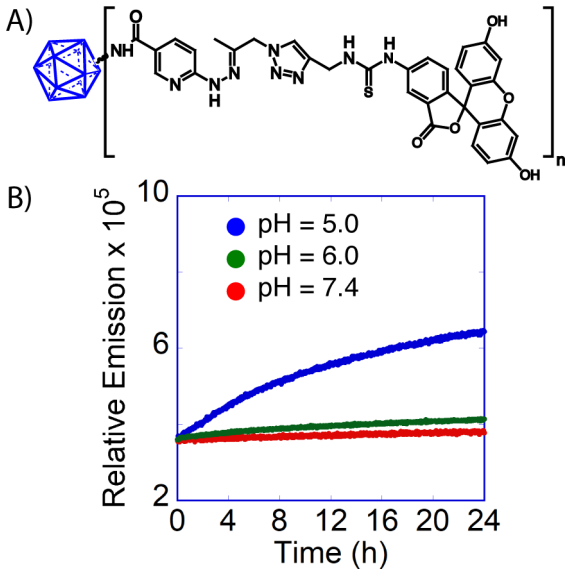

Figure 4. (A) Qβ-ZFITC was used for the kinetics studies. (B) Release profiles of FITC from Qβ-ZFITC at pH 7.4 (KP buffer, 0.1 M, 25 °C), pH 6.0 (MES buffer, 0.1 M, 25 °C), and pH 5.0 (MES buffer, 0.1 M, 25 °C).

high local concentrations[48,49] while conjugated to the capsid. As the hydrolysis proceeds, releasing FITC into the solution, the increase in fluorescence can be monitored over time. We tracked the release of FITC from the VLP into solutions at a pH of 7.4, 6.0, and 5.0. The maximum fluorescence was seen after 24 h at pH 5.0, while very small increases in fluorescence were observed over the same time period for the conjugates incubated at pH 7.4 and 6.0 (Figure 4b). When the fluorescence values were fit to a pseudo-first-order reaction model, the half-lives of hydrazone hydrolysis at pH 7.4, 6.0, and 5.0 were 21.3, 9.6, and 6.4 h, respectively. The observed kinetics results are consistent with the expected hydrolysis properties of the hydrazone linker. While these half-lives are likely too long for therapeutic use, we have confirmed the chemistry works. The question of the extent of hydrolysis is still pending, but it is obvious that hydrolysis is occurring by the change in fluorescence, the identification of the predicted mass by MALDI-TOF, and the difference in electrophoretic mobility.

Finally, we turned to in vitro studies to determine the efficacy of our strategy. Flow cytometry and fluorescence microscopy were used to evaluate the cell uptake efficiency of the Qβ conjugates. Phagocytic cells have been shown to favor the uptake of negatively charged nanoparticles, so their use in probing the uptake characteristics of the different Qβ conjugates could advance the understanding of the mechanisms behind the uptake selectivity of phagocytic cells. RAW 264.7 macrophages and HeLa cells were incubated in cell media containing 10% serum with their respective Qβ conjugates for 4 h. The concentrations of the Qβ conjugates ranged from 10 to 50 μM relative to the coat protein. A comparison of the cell uptake efficiency by flow cytometry of the Qβ-ZX conjugate and its hydrolyzed form, Qβ-ZX-Hyd, is shown in Figure 5a,b. When both cell lines were incubated with the Qβ conjugates at 10 μM, no significant changes in the fluorescence intensities of the cells were observed, even for the unfunctionalized Q$\beta_{(GFP)}$ positive control. This result suggests that the concentration of Qβ conjugates used for incubation were too low for the detection of fluorescence. When both cell lines were incubated with the Qβ conjugates at 50 μM, significant differences in the fluorescence intensities of cell populations were observed. The RAW 264.7 macrophages incubated with 50 μM Qβ-ZX-Hyd displayed a noticeable increase in fluorescence intensity, while the macrophages incubated with 50 μM Qβ-ZX did not. This suggests that the macrophages have internalized the positively charged Qβ-ZX-Hyd conjugate. We wanted to see if these results were specific to the macrophages, so we tested them on HeLa cells, which were incubated with Qβ conjugates at 50 μM. Although HeLa cells incubated with 50 μM Qβ-ZX-Hyd displayed a clear increase in fluorescence intensity while the cells incubated with 50 μM Qβ-ZX did not, the magnitude of the increase in fluorescence intensity is far lower than what is observed for the RAW 264.7 macrophages. This is expected because macrophages are commonly known to internalize a wide array of foreign materials due to their role as phagocytes.[7,9,11,50,51] These results are further illustrated in Figure 5c,d by fluorescence imaging, showing the internalization of the Qβ-ZX-Hyd conjugates yet zero internal fluorescence of Qβ-ZX. We repeated these tests on the Qβ-ZX2 conjugate, which has a longer linker between the VLP and the hexanoic acid (see Scheme 2), and found the same results from flow cytometry. This result also corroborates our hypothesis that the linker between the VLP and the hexanoic acid moiety can be altered without changing the structure—

DOI: 10.1021/acs.molpharmaceut.8b00348
Mol. Pharmaceutics XXXX, XXX, XXX−XXX

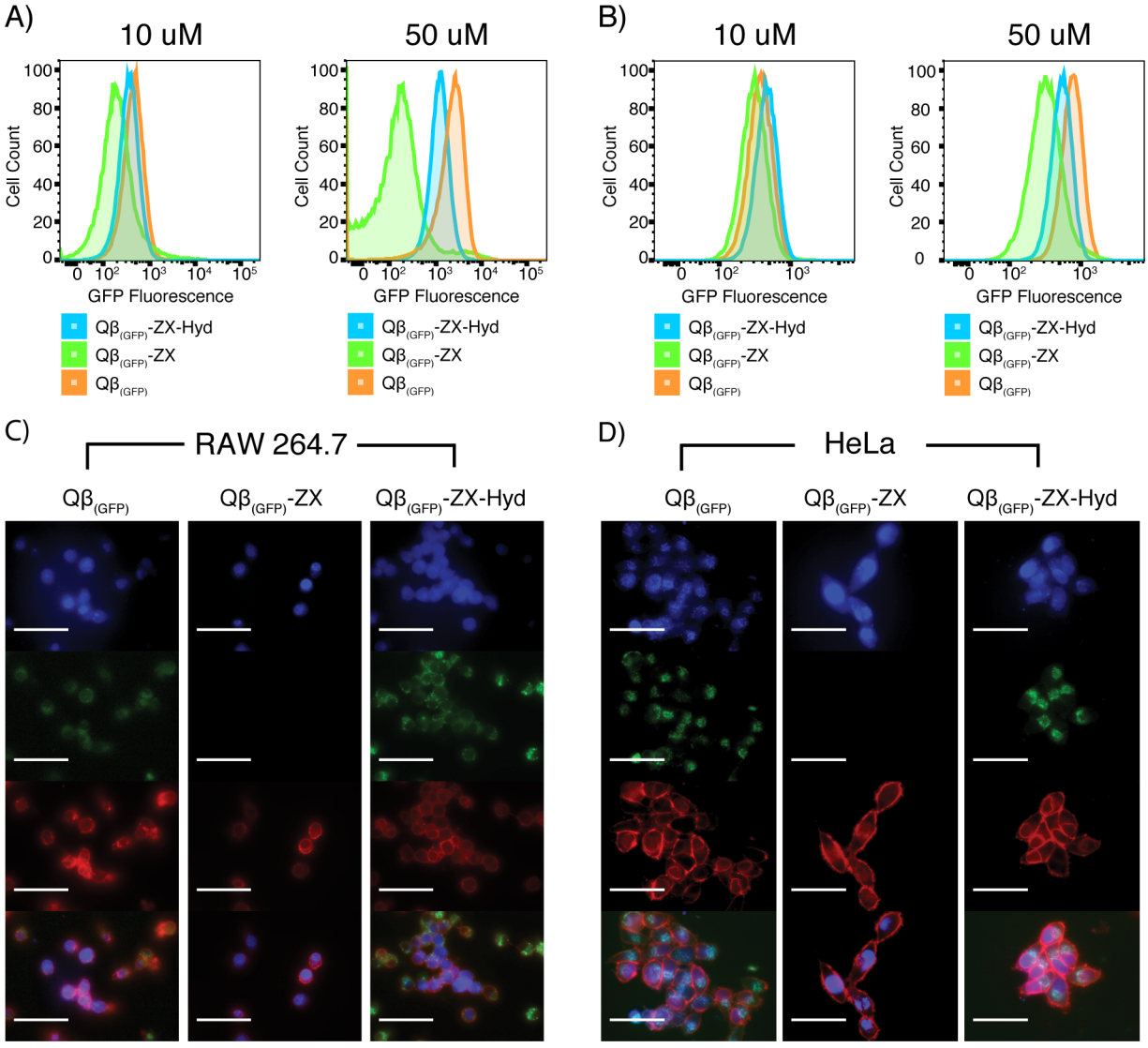

Figure 5. Representative histograms from flow cytometry studies corresponding to (A) RAW 264.7 macrophages and (B) HeLa cells incubated with their respective Qβ samples. Epifluorescence microscope images of (C) RAW 264.7 macrophages and (D) HeLa cells incubated with their respective Qβ samples (50 μM). Blue: DAPI; red: WGA-AlexaFluor 555; and green: GFP. Scale bar represents 50 μm. All cells were incubated with the QB conjugates for 4 h at 37 °C.

function properties. We anticipate that other linker designs, for instance, ones that are cleavable by enzymatic activity or light, are likely also able to be tolerated and, as such, expand on the generalizability of this approach.

CONCLUSIONS

We have shown that conjugating terminal hexanoic acid moieties onto the surface of VLP Qβ inhibits the uptake of the conjugate by RAW 264.7 macrophages and HeLa cells. Installing hydrazone linkers between the surface of Qβ and the terminal alkyl carboxylate moieties results in a pH-responsive conjugate that, in acidic conditions, can release the terminal hexanoic acid moiety and allow for the uptake of the Qβ nanoparticle. Importantly, the installation of the "pH switch" did not change the structure–function properties of the hexanoic acid linker. Collectively, these findings are a helpful reminder that, even when the size and shape of nanoparticles are controlled for, charge alone does not always account for its uptake characteristics by both macrophages and HeLa cells. In addition, these findings highlight the need for further studies to advance the understanding of the requirements necessary to design effective nanoparticle-based systems for the delivery of payloads into cells.

ASSOCIATED CONTENT

Supporting Information

The Supporting Information is available free of charge on the ACS Publications website at DOI: 10.1021/acs.molpharmaceut.8b00348.

Detailed experimental and synthetic procedures, characterization of small molecules, Qβ expression and purification protocols, bioconjugation protocols, cell cultures, and instrumentation (PDF)

AUTHOR INFORMATION

Corresponding Author

*E-mail: gassensmith@utdallas.edu.

DOI: 10.1021/acs.molpharmaceut.8b00348
Mol. Pharmaceutics XXXX, XXX, XXX−XXX

ORCID

Hamilton Lee: 0000-0003-2176-925X
Candace E. Benjamin: 0000-0002-9211-718X
Lana H. Tuong: 0000-0002-8124-7827
Raymond P. Welch: 0000-0003-3114-8801
Zhuo Chen: 0000-0001-7775-7579
Madushani Dharmarwardana: 0000-0002-3086-047X
Kyle W. Murray: 0000-0002-2567-1703
Jeremiah J. Gassensmith: 0000-0001-6400-8106

Author Contributions

⊥H.L. and C.E.B. contributed equally to this work.

Funding

J.J.G. acknowledges the National Science Foundation (DMR-1654405) and the Cancer Prevention and Research Institute of Texas (CPRIT) (RP170752) for their support.

Notes

The authors declare no competing financial interest.

REFERENCES

(1) Elsabahy, M.; Wooley, K. L. Nanoparticles for Biomedical Delivery Applications. *Chem. Soc. Rev.* **2012**, *41* (7), 2545−2561.

(2) Yoon, H. Y.; Jeon, S.; You, D. G.; Park, J. H.; Kwon, I. C.; Koo, H.; Kim, K. Inorganic Nanoparticles for Image-Guided Therapy. *Bioconjugate Chem.* **2017**, *28* (1), 124−134.

(3) Zhang, N.; Zhao, F.; Zou, Q.; Li, Y.; Ma, G.; Yan, X. Multitriggered Tumor-Responsive Drug Delivery Vehicles Based on Protein and Polypeptide Coassembly for Enhanced Photodynamic Tumor Ablation. *Small* **2016**, *12* (43), 5936−5943.

(4) Abbas, M.; Zou, Q.; Li, S.; Yan, X. Self-Assembled Peptide- and Protein-Based Nanomaterials for Antitumor Photodynamic and Photothermal Therapy. *Adv. Mater.* **2017**, *29* (12), 1605021.

(5) Li, X.; Che, Z.; Mazhar, K.; Price, T. J.; Qin, Z. Ultrafast Near-Infrared Light-Triggered Intracellular Uncaging toProbe Cell Signaling. *Adv. Funct. Mater.* **2017**, *27* (11), 1605778.

(6) Salatin, S.; Maleki Dizaj, S.; Yari Khosroushahi, A. Effect of the surface modification, size, and shape on cellular uptake of nanoparticles. *Cell Biol. Int.* **2015**, *39* (8), 881−90.

(7) Frohlich, E. The role of surface charge in cellular uptake and cytotoxicity of medical nanoparticles. *Int. J. Nanomed.* **2012**, *7*, 5577−91.

(8) Blanco, E.; Shen, H.; Ferrari, M. Principles of nanoparticle design for overcoming biological barriers to drug delivery. *Nat. Biotechnol.* **2015**, *33* (9), 941−951.

(9) Walkey, C. D.; Olsen, J. B.; Guo, H.; Emili, A.; Chan, W. C. Nanoparticle size and surface chemistry determine serum protein adsorption and macrophage uptake. *J. Am. Chem. Soc.* **2012**, *134* (4), 2139−47.

(10) Lesniak, A.; Salvati, A.; Santos-Martinez, M. J.; Radomski, M. W.; Dawson, K. A.; Aberg, C. Nanoparticle adhesion to the cell membrane and its effect on nanoparticle uptake efficiency. *J. Am. Chem. Soc.* **2013**, *135* (4), 1438−44.

(11) He, C.; Hu, Y.; Yin, L.; Tang, C.; Yin, C. Effects of particle size and surface charge on cellular uptake and biodistribution of polymeric nanoparticles. *Biomaterials* **2010**, *31* (13), 3657−66.

(12) Cheng, X.; Tian, X.; Wu, A.; Li, J.; Tian, J.; Chong, Y.; Chai, Z.; Zhao, Y.; Chen, C.; Ge, C. Protein Corona Influences Cellular Uptake of Gold Nanoparticles by Phagocytic and Nonphagocytic Cells in a Size-Dependent Manner. *ACS Appl. Mater. Interfaces* **2015**, *7* (37), 20568−75.

(13) Sanchez-Moreno, P.; Buzon, P.; Boulaiz, H.; Peula-Garcia, J. M.; Ortega-Vinuesa, J. L.; Luque, I.; Salvati, A.; Marchal, J. A. Balancing the effect of corona on therapeutic efficacy and macrophage uptake of lipid nanocapsules. *Biomaterials* **2015**, *61*, 266−278.

(14) Key, J.; Palange, A. L.; Gentile, F.; Aryal, S.; Stigliano, C.; Di Mascolo, D.; De Rosa, E.; Cho, M.; Lee, Y.; Singh, J.; Decuzzi, P. Soft Discoidal Polymeric Nanoconstructs Resist Macrophage Uptake and Enhance Vascular Targeting in Tumors. *ACS Nano* **2015**, *9* (12), 11628−11641.

(15) Orellana-Tavra, C.; Haddad, S.; Marshall, R. J.; Lazaro, I. A.; Boix, G.; Imaz, I.; Maspoch, D.; Forgan, R. S.; Fairen-Jimenez, D. Tuning the Endocytosis Mechanism of Zr-Based Metal−Organic Frameworks through Linker Functionalization. *ACS Appl. Mater. Interfaces* **2017**, *9* (41), 35516−35525.

(16) Nel, A. E.; Madler, L.; Velegol, D.; Xia, T.; Hoek, E. M.; Somasundaran, P.; Klaessig, F.; Castranova, V.; Thompson, M. Understanding biophysicochemical interactions at the nano-bio interface. *Nat. Mater.* **2009**, *8* (7), 543−57.

(17) Lee, C. H.; Cheng, S. H.; Huang, I. P.; Souris, J. S.; Yang, C. S.; Mou, C. Y.; Lo, L. W. Intracellular pH-responsive mesoporous silica nanoparticles for the controlled release of anticancer chemotherapeutics. *Angew. Chem., Int. Ed.* **2010**, *49* (44), 8214−9.

(18) Zhang, F.; Correia, A.; Makila, E.; Li, W.; Salonen, J.; Hirvonen, J. J.; Zhang, H.; Santos, H. A. Receptor-Mediated Surface Charge Inversion Platform Based on Porous Silicon Nanoparticles for Efficient Cancer Cell Recognition and Combination Therapy. *ACS Appl. Mater. Interfaces* **2017**, *9* (11), 10034−10046.

(19) Mosquera, J.; Henriksen-Lacey, M.; Garcia, I.; Martinez-Calvo, M.; Rodriguez, J.; Mascarenas, J. L.; Liz-Marzan, L. M. Cellular Uptake of Gold Nanoparticles Triggered by Host-Guest Interactions. *J. Am. Chem. Soc.* **2018**, *140* (13), 4469.

(20) Dempsey, C.; Lee, I.; Cowan, K. R.; Suh, J. Coating barium titanate nanoparticles with polyethylenimine improves cellular uptake and allows for coupled imaging and gene delivery. *Colloids Surf., B* **2013**, *112*, 108−112.

(21) Suk, J. S.; Suh, J.; Choy, K.; Lai, S. K.; Fu, J.; Hanes, J. Gene delivery to differentiated neurotypic cells with RGD and HIV Tat peptide functionalized polymeric nanoparticles. *Biomaterials* **2006**, *27* (29), 5143−5150.

(22) Yue, Z.-G.; Wei, W.; Lv, P.-P.; Yue, H.; Wang, L.-Y.; Su, Z.-G.; Ma, G.-H. Surface Charge Affects Cellular Uptake and Intracellular Trafficking of Chitosan-Based Nanoparticles. *Biomacromolecules* **2011**, *12* (7), 2440−2446.

(23) Corpe, W. A. Attachment of Marine Bacteria to Solid Surfaces. In *Adhesion in Biological Systems*; Manly, R., Ed.; Academic Press: New York, 1970.

(24) Brown, M. S.; Basu, S. K.; Falck, J. R.; Ho, Y. K.; Goldstein, J. L. The scavenger cell pathway for lipoprotein degradation: Specificity of the binding site that mediates the uptake of negatively-charged LDL by macrophages. *J. Supramol. Struct.* **1980**, *13* (1), 67−81.

(25) Gustafson, H. H.; Holt-Casper, D.; Grainger, D. W.; Ghandehari, H. Nanoparticle uptake: The phagocyte problem. *Nano Today* **2015**, *10* (4), 487−510.

(26) Salis, A.; Fanti, M.; Medda, L.; Nairi, V.; Cugia, F.; Piludu, M.; Sogos, V.; Monduzzi, M. Mesoporous Silica Nanoparticles Functionalized with Hyaluronic Acid and Chitosan Biopolymers. Effect of Functionalization on Cell Internalization. *ACS Biomater. Sci. Eng.* **2016**, *2* (5), 741−751.

(27) Kruse, C. R.; Singh, M.; Targosinski, S.; Sinha, I.; Sorensen, J. A.; Eriksson, E.; Nuutila, K. The effect of pH on cell viability, cell migration, cell proliferation, wound closure, and wound reepithelialization: In vitro and in vivo study. *Wound Repair Regen* **2017**, *25* (2), 260−269.

(28) Percival, S. L.; McCarty, S.; Hunt, J. A.; Woods, E. J. The effects of pH on wound healing, biofilms, and antimicrobial efficacy. *Wound Repair Regen* **2014**, *22* (2), 174−86.

(29) Gethin, G. The significance of surface pH in chronic wounds. *Wound Healing Science* **2007**, *3* (3), 52−56.

(30) Pokorski, J. K.; Breitenkamp, K.; Liepold, L. O.; Qazi, S.; Finn, M. G. Functional virus-based polymer-protein nanoparticles by atom transfer radical polymerization. *J. Am. Chem. Soc.* **2011**, *133* (24), 9242−5.

(31) Wen, A. M.; Steinmetz, N. F. Design of Virus-based Nanomaterials for Medicine, Biotechnology, and Energy. *Chem. Soc. Rev.* **2016**, *45* (15), 4074−4126.

DOI: 10.1021/acs.molpharmaceut.8b00348
Mol. Pharmaceutics XXXX, XXX, XXX−XXX

(32) Chen, Z.; Li, N.; Li, S.; Dharmarwardana, M.; Schlimme, A.; Gassensmith, J. J. Viral Chemistry: The Chemical Functionalization of Viral Architectures to Create New Technology. *WIREs Nanomed. Nanobiotechnol.* **2016**, *8* (4), 512−534.
(33) Yildiz, I.; Shukla, S.; Steinmetz, N. F. Applications of Viral Nanoparticles in Medicine. *Curr. Opin. Biotechnol.* **2011**, *22* (6), 901−908.
(34) Koudelka, K. J.; Pitek, A. S.; Manchester, M.; Steinmetz, N. F. Virus-Based Nanoparticles as Versatile Nanomachines. *Annu. Rev. Virol.* **2015**, *2* (1), 379−401.
(35) Lee, K. L.; Shukla, S.; Wu, M.; Ayat, N. R.; El Sanadi, C. E.; Wen, A. M.; Edelbrock, J. F.; Pokorski, J. K.; Commandeur, U.; Dubyak, G. R.; Steinmetz, N. F. Stealth Filaments: Polymer Chain Length and Conformation Affect the in vivo Fate of PEGylated Potato Virus X. *Acta Biomater.* **2015**, *19*, 166−179.
(36) Longmire, M.; Choyke, P. L.; Kobayashi, H. Clearance Properties of Nano-sized Particles and Molecules as Imaging Agents: Considerations and Caveats. *Nanomedicine* **2008**, *3* (5), 703−717.
(37) Zeltins, A. Construction and Characterization of Virus-Like Particles: A Review. *Mol. Biotechnol.* **2013**, *53* (1), 92−107.
(38) Golmohammadi, R.; Fridborg, K.; Bundule, M.; Valegård, K.; Liljas, L. The crystal structure of bacteriophage Qβ at 3.5 å resolution. *Structure* **1996**, *4* (5), 543−554.
(39) Chen, Z.; Li, N.; Chen, L.; Lee, J.; Gassensmith, J. J. Dual Functionalized Bacteriophage Qbeta as a Photocaged Drug Carrier. *Small* **2016**, *12* (33), 4563−71.
(40) Grayson, E. J.; Bernardes, G. J. L.; Chalker, J. M.; Boutureira, O.; Koeppe, J. R.; Davis, B. G. A Coordinated Synthesis and Conjugation Strategy for the Preparation of Homogeneous Glycoconjugate Vaccine Candidates. *Angew. Chem., Int. Ed.* **2011**, *50* (18), 4127−4132.
(41) Jin, A. J.; Mertz, D.; Liao, H.-S.; Johri, A.; Torres, L.; Wu, Y.; Narum, D. Quantifying Nanoscale Properties of Engineered Virus Capsids for Malaria Vaccines. *Biophys. J.* **2016**, *110* (3), 171a.
(42) Rhee, J.-K.; Fiedler, J. D.; Brown, S. D.; Manzenrieder, F.; Kitagishi, H.; Nycholat, C.; Paulson, J. C.; Finn, M. G.; Hovlid, M. Colorful Virus-Like Particles: Fluorescent Protein Packaging by the Qβ Capsid. *Biomacromolecules* **2011**, *12* (11), 3977−3981.
(43) Sato, M.; Hiragun, A.; Shudo, K. Functional studies of newly synthesized benzoic acid derivatives: Identification of highly potent retinoid-like activity. *J. Cell. Physiol.* **1988**, *135* (2), 179−188.
(44) Xu, C.; Tian, H.; Sun, H.; Jiao, Z.; Zhang, Y.; Chen, X. A pH sensitive co-delivery system of siRNA and doxorubicin for pulmonary administration to B16F10 metastatic lung cancer. *RSC Adv.* **2015**, *5* (125), 103380−103385.
(45) Kalia, J.; Raines, R. T. Hydrolytic stability of hydrazones and oximes. *Angew. Chem., Int. Ed.* **2008**, *47* (39), 7523−6.
(46) Wallat, J. D.; Harrison, J. K.; Pokorski, J. K. pH Responsive Doxorubicin Delivery by Fluorous Polymers for Cancer Treatment. *Mol. Pharmaceutics* **2018**, 1.
(47) Jończyk, E.; Kłak, M.; Międzybrodzki, R.; Górski, A. The influence of external factors on bacteriophages—review. *Folia Microbiol.* **2011**, *56* (3), 191−200.
(48) Sato, D.; Kato, T. Novel fluorescent substrates for detection of trypsin activity and inhibitor screening by self-quenching. *Bioorg. Med. Chem. Lett.* **2016**, *26* (23), 5736−5740.
(49) Munkholm, C.; Walt, D. R.; Parkinson, D. R. Intramolecular Fluorescence Self-Quenching of Fluoresceinamine. *J. Am. Chem. Soc.* **1990**, *112* (7), 2608−2612.
(50) Olsson, M.; Nilsson, A.; Oldenborg, P. A. Dose-dependent inhibitory effect of CD47 in macrophage uptake of IgG-opsonized murine erythrocytes. *Biochem. Biophys. Res. Commun.* **2007**, *352* (1), 193−7.
(51) Okazawa, H.; Motegi, S.; Ohyama, N.; Ohnishi, H.; Tomizawa, T.; Kaneko, Y.; Oldenborg, P. A.; Ishikawa, O.; Matozaki, T. Negative regulation of phagocytosis in macrophages by the CD47-SHPS-1 system. *J. Immunol.* **2005**, *174* (4), 2004−11.

DOI: 10.1021/acs.molpharmaceut.8b00348
Mol. Pharmaceutics XXXX, XXX, XXX−XXX